Computational study on the roles of amino acid residues in the active site formation mechanism of blue-light photoreceptors

Ryuma Sato[1], Hirotaka Kitoh-Nishioka[2], Koji Ando[3], Takahisa Yamato[1*]

1. *Department of Physics, Graduate School of Science, Nagoya University, Furo-cho, Chikusa-ku, Nagoya 464-8602, Japan*
2. *Department of Chemistry, Graduate School of Science, Nagoya University, Furo-cho, Chikusa-ku, Nagoya 464-8602, Japan*
3. *Department of Chemistry, Graduate School of Science, Kyoto University, Kitashirakawa-Oiwake-cho, Sakyo-ku, Kyoto 606-8502, Japan*

* Correspondence: yamato@nagoya-u.jp

Abstract

To examine the functional roles of the active site methionine (M-site) and glutamic acid (E-site) residues of blue-light photoreceptors, we performed *in silico* mutation at the M-site in a systematic manner and focused on the hydrogen bonding between the E-site and the substrate: the cyclobutane pyrimidine dimer (CPD). Fragment molecular orbital calculations with electron correlations demonstrated that substitution of the M-site methionine with either alanine or glutamine always destabilizes the interaction energy between the E-site and the CPD by more than 12.0 kcal/mol, indicating that the methionine and glutamic acid residues cooperatively facilitate the enzymatic reaction in the active site.

Introduction

The cyclobutane pyrimidine dimer (CPD), which is formed between two adjacent pyrimidines [1], is the most abundant among the various genotoxic photoproducts in DNA. The enzyme CPD photolyase (PHR) repairs CPDs through an electron transfer (ET) reaction induced by the absorption of blue light [2], [3], [4] by a flavin adenine dinucleotide ($FADH^{-}$) cofactor, which subsequently donates one electron to the CPD (Fig. 1). It has been proposed that the CPD anion radical is stabilized by transient proton transfer from a nearby glutamic acid residue (hereafter denoted the E-site) that is hydrogen bonded to the CPD [5][6]. Repair of the CPD lesion is completed with the opening of the CPD ring and return of the electron from the repaired anionic thymine to $FADH^{\bullet}$. A number of theoretical and experimental studies have been conducted on the enzymatic reaction mechanism of PHR. Nevertheless, there are still ongoing debates concerning the details of the molecular mechanism.

Theoretical calculations [7–10] have been used to investigate electron tunneling pathways for the abovementioned ET reaction. One model suggested a major route via an intervening adenine moiety, involving an extraordinary U-shaped cofactor [7], [8]. This model is consistent with spectroscopic measurements [11]. Another model concluded that the electron travels directly through space from the donor to the acceptor [9], [10]. A computational study that focused on the roles of amino acid residues suggested that the ET reaction catalyzed by the Class I CPD photolyase (Phr1) derived from *A. nidulans* is facilitated by the methionine residue at position 353 (hereafter denoted as M-site) [12]. To evaluate the effect of thermal fluctuations, 10000 conformations were extracted from the molecular dynamics trajectory of Phr1, and then extended-Hückel calculations were performed using these conformations. The level of the computations may not have been accurate enough for quantitative evaluation of the electron transfer rate. Nevertheless, a bioinformatics analysis demonstrated that the methionine residue at the M-site is 100% conserved in the Phr1 family. This observation indicates that the M-site methionine plays a critical role in the enzymatic function of Phr1.

The roles of active site residues have been investigated in experimental studies. Using femtosecond spectroscopy and site-directed mutagenesis, Liu et al. studied the reaction dynamics of wild-type PHR and its mutants with different substrates [13]. They demonstrated that an alanine mutation at the E-site residue led to a significantly

decreased quantum yield for the reaction (0.40), compared with that of the wild-type (0.82). Since the glutamic acid residue at position 283 (E-site) forms two hydrogen bonds with the 5'side of the CPD (Fig.2), it is likely that the residue plays a central role in active site stabilization. It is proposed, as mentioned above, that a transient proton transfer occurs in the active site during the repair cycle of CPD. If this is the case, the E-site glutamic acid may also serve as a possible proton donor to the anionic intermediate of CPD [5][6].

It is interesting to note that the cryptochrome (Cry) and photolyase (Phr) families have very different biological functions, despite sharing high degrees of sequence identity and structural similarity between them. From a structural point of view, there is no doubt that the enzymatic activity of Phr1 is particularly sensitive to the fine-tuning of its active site conformation. Recently, an X-ray crystal structure of the complex of cryptochrome DASH (Cry-DASH) with a single-stranded DNA containing a CPD lesion was reported [14]. Although the structure of Cry-DASH (so-named for its presence in *Drosophila*, *Arabidopsis*, *Synechocystis*, and *Homo*) is strikingly similar to that of Phr, the biological function of Cry-DASH is still not completely known. A role in the control of transcription was indicated by an *in vivo* experiment [15], while an *in vitro* study provided evidence that Cry-DASH has a role in light-induced single-stranded DNA repair [16]. An active-site comparison of Phr1 with Cry-DASH would provide some structural clues about the reaction mechanism of Phr1. The active site of *A. nidulans* Phr1 comprises Arg-232, Glu-283, Trp-286, Asn-349, Met-353, and Trp-392, while that of *Arabidopsis thaliana* Cry-DASH comprises Arg-276, Glu-325, Trp-328, Asn-391, Gln-395, and Tyr-434 [17]. We see that Met-353 and Trp-392 of Phr1 are replaced by glutamine and tyrosine, respectively, in Cry-DASH.

Computational studies will be helpful to ongoing efforts to elucidate the molecular mechanism of DNA repair by Phr1. In this study, we focus on the roles of the E-site and M-site residues of Phr1. Using molecular dynamics and quantum chemistry calculations, we analyzed the structural fluctuation and stability of the active sites of wild-type Phr1 ($Phr1^{wild}$), Phr1 mutants, wild-type Cry-DASH ($Cry\text{-}DASH^{wild}$), and Cry-DASH mutants, respectively. We performed *in silico* mutations of the M-site methionine (Met-353) in Phr1 to alanine or glutamine, as well as mutations of the M-site glutamine in Cry-DASH (Gln-395) to alanine or methionine. Furthermore, we performed fragment molecular orbital calculations at the second order Møller-Plesset perturbation level, and

compared the energetic stabilities of the active sites of Phr1^{wild}, Phr1^{M353A}, Phr1^{M353Q}, Cry-DASH^{wild}, Cry-DASH^{Q395A}, and Cry-DASH^{Q395M} in a systematic manner.

Materials and Method

Model building

The atomic coordinates of *A. nidulans* Phr1 complexed with a CPD analogue (PDB ID code: 1TEZ [18]) and *Arabidopsis thaliana* Cry-DASH (PDB ID code: 2VTB [17]) were derived from the RCSB Protein Data Bank's X-ray crystallographic database. These models were denoted Phr1^{wild} and Cry-DASH^{wild}, respectively. For Phr1^{wild} (Cry-DASH^{wild}), we introduced single amino acid substitutions at the M-site methionine (glutamine) to either alanine or glutamine (alanine or methionine), using the Winmoster program [19]. The protonation states of the titratable amino acid residues were kept in their standard states at pH 7, except for the glutamic acid on the E-site, which was protonated [13] in each model. To build a CPD analogue model, the atomic coordinates were extracted from the NMR structure (PDB ID code: 1SNH [20]), and the–O–P_2–O– part was replaced with–O–CH_2–O–. Thus, we obtained six models: (A) Phr1^{wild}, (B) Phr1^{M353Q}, (C) Phr1^{M353A}, (D) Cry-DASH^{wild}, (E) Cry-DASH^{Q395M}, and (F) Cry-DASH^{Q395A}. Each model included crystallographic waters, and was then immersed in an octahedral box of water molecules, where the number of water molecules were 25258, 25258, 25257, 25385, 25385, and 25387, respectively. The TIP3P model [21] was employed for the water molecules. The total number of atoms per unit cell became 84033, 84033, 84023, 84538, 84538, and 84537, respectively.

Molecular dynamics simulation

We performed molecular dynamics (MD) simulations for each model using the Amber 12 program [22] with ff12SB force-field functions. The partial atomic charges for the protein atoms were assigned using the tLEaP program, while those of the singlet ground states of the CPD analogue, a fully reduced flavin-adenine-dinucleotide ($FADH^-$), 8-hydroxy-5-deazaflavin (8-HDF), and 5, 10-methylenetetrahydrofolate (MTHF) were determined using the RESP method, which was implemented using the Antechamber module, based on *ab initio* molecular orbital calculations at the restricted Hartree-Fock level with 6-31G(d) basis set, in Gaussian 03 [23]. For nonstandard

residues or co-factors, assignment of atom types and selection of bonded parameters were done by the antechamber module. Force-filed files for these groups are available via the Internet (http://www.comp-biophys.com/yamato-lab/resources.html). Missing parameters were derived from the amber parameter database (http://personalpages.manchester.ac.uk/staff/Richard.Bryce/amber/cof/FADH-.frcfld).

Before sampling of the conformation, the initial structure of each of the six models was optimized by imposing harmonic restraints on all nonhydrogen atoms, except for the solvent water molecules, using a force constant of 100 (kcal/mol)/Å^2. Then, another energy minimization was performed without any positional restraints. After that, a 20-ps NVT molecular dynamics simulation was conducted, during which the temperature of the system was elevated from 0 K to 300 K, while harmonic restraints were imposed on all nonhydrogen atoms using a force constant of 10 (kcal/mol)/Å^2. Next, thermal equilibration was achieved after a 5-ns NVT simulation at T = 300 K without harmonic restraints. Finally, another 5-ns NPT simulation was continued to obtain a canonical ensemble at T = 300 K and P = 1 atm. The molecular dynamics calculations were performed employing an octahedral periodic boundary condition with the particle mesh Ewald method, using a time step of 1 fs for the integration of equations of motions.

Molecular orbital calculations

Ab initio quantum chemical (QM) calculations were performed using the two-body fragment molecular orbital (FMO2) method with electron correlations from the second-order Møller-Plesset (MP2) perturbation theory [24], [25], [26], [27], [28]. The 6-31G(d) basis set was employed. In the FMO-MP2 method, the total system was divided into fragments, and then the one- and two-body QM energies of the fragments were determined self-consistently within the Coulomb field created by the other fragments.

For each of the six models, 100 instantaneous structures of the molecular mechanics (MM) model were extracted from the MD trajectories. As shown in Figure 3, the QM models of the Phr1s (Cry-DASHs) were constructed based on these MM models, in which QM regions comprised the flavin mononucleotide; the adenine; the CPD (see Figs. S1, S2); and the protonated-Glu283 (325), Trp286 (328), Asn349 (391), Arg352 (394) and adenine moieties; together with the M-site residue: Met353, Ala353, Gln353,

Gln395, Ala395, and Met395 for Phr1^{wild}, Phr1^{M353A}, Phr1^{M353Q}, Cry-DASH^{wild}, Cry-DASH^{Q395A}, and Cry-DASH^{Q395M}, respectively. In the QM regions, the main chain NH and CO groups were replaced by hydrogen atoms. We used the GAMESS program [29] for the FMO-MP2 calculations of the QM regions in a vacuum environment. Using preliminary calculations, we confirmed that the influence of the surrounding environment on the electronic state of the QM region was negligible.

Results and Discussion

Hydrogen bond formation between the E-site glutamic acid and the CPD

For each of the six models, we examined the stability of the hydrogen bond between the CPD and the E-site Glu during the MD simulations. Fig. 4 shows that the distance between the CPD and the E-site Glu is the shortest for Phr1^{wild} (Cry-DASH^{Q395M}) among the three Phr1s (Cry-DASHs), indicating that the M-site methionine facilitates the formation of a strong hydrogen bond formation the CPD and the E-site (Fig. 5).

Interaction between the M-site residue and the CPD

Next, we examined the distance between the CPD and the M-site residue for each of the six models (Fig. 6, 7). For both of the Phr1s and the Cry-DASHs, the distance is the shortest, second shortest, and largest when the M-site residue is glutamine, methionine, and alanine, respectively (Fig. 7). This indicates that the interaction between the M-site glutamine (alanine) and CPD is too strong (weak) for stable hydrogen bonding between the CPD and the E-site Glu, while an M-site methionine allows the CPD to maintain an appropriate distance from the E-site Glu. To analyze the energetics of the active site formation mechanism in a quantitative manner, we performed *ab initio* molecular orbital calculations.

The Interaction energy between the CPD and the surrounding protein environment

The FMO2-MP2/6-31G(d) calculations were used to determine the interfragment interaction energy between the CPD and the surrounding amino acid residues for each of the six models (Table I). The interaction energy between CPD and the E-site Glu was the lowest for Phr1^{wild} (Cry-DASH^{Q395M}) among the three Phr1s (Cry-DASHs),

indicating that the M-site methionine facilitates the formation of a stable hydrogen bond between the CPD and the glutamic acid residue.

Functional importance of the interactions between the E-site and CPD

According to the experimental study[13], the photorepair cycle of the CPD triggered by the initial light absorption consists of the following steps: (1) The forward electron transfer (FET) from the photoexcited $FADH^{-*}$ to CPD (250 ps), (2) C5–C5' splitting (<10 ps), (3) C6–C6' splitting (90 ps), (4) Electron return (ER) to the FADH radical (700 ps), where the time constant is indicated in parenthesis for each step. There is a possibility that a back electron transfer (BET) reaction occurs from the CPD anion radical to the FADH radical after the second step. In such a case, the repair cycle will not be completed. For the wild-type, a large time constant of the BET (2.4 ns) ensures successful C6–C6' splitting before the intermediate state is lost due to the BET. For the E274 mutant, contrastingly, the time constant of BET is approximately 50 ps, while that of C6-C6' splitting is 30 ps. In this case, the intermediate state after the second step may partly return to the initial state by the BET reaction. As a result, the quantum yield of the E274 photorepair cycle is significantly decreased to 0.40 from that of the wild-type (0.82). Obviously, the E274A mutant cannot form any hydrogen bond between the E-site alanine and CPD. Therefore, the hydrogen bonding between the E-site and CPD, which may be associated with the large time constant of the wild-type BET, is an important factor for the efficient repair reaction of the enzyme.

From the point of view of the molecular mechanism, it is possible that a proton transfer takes place from the E-site glutamic acid to the CPD anion radical, which was indicated in the literature [6]. They performed first-principles molecular dynamics simulations, and observed proton transfer five times out of the seven trials, indicating that the transferred proton stabilizes the transient CPD anion radical state during the reaction cycle and facilitates efficient repair reaction. Obviously, stable hydrogen bonding is favorable for proton transfer reactions. However, we should be aware that there has been no direct experimental evidence for the occurrence of proton transfer during the repair cycle. Further studies are needed to elucidate the molecular mechanism of the repair cycle in more detail.

Conclusions

Molecular dynamics simulations and molecular orbital calculations demonstrated that the active site methionine residue (M-site) of CPD photolyase facilitates stable hydrogen bonding between the active site glutamic acid (E-site) and the CPD, indicating that these two sites cooperatively maintain the active site conformation suitable for the efficient DNA repair cycle, because the E-site glutamic acid is known to be an important factor for the repair cycle with high quantum yield.

Acknowledgements

The work was supported by a MEXT Grant-in-Aid for Scientific Research on Innovative Areas (#22104009) to T.Y. The computations were performed at the computer centers of Nagoya University, and the Okazaki Research Center for Computational Sciences. This research is partially supported by the Collaborative Research Program for Young Scientists of ACCMS and IIMC, Kyoto University.

Table I. Interactions between the CPD substrate and the active site components

	E283	W285	N349	M (Q, A) 353	FMN	Adenine
$Phr1^{wild}$	−16.6156 ±3.9956 (0.0)	−13.6578 ±1.5912 (0.0)	−15.0824 ±3.1109 (0.0)	−8.0568 ±1.3001 (0.0)	5.7623 ±1.1792 (0.0)	−6.5553 ±1.1034 (0.0)
$Phr1^{M353Q}$	0.1846 ±0.5174 (16.4310)	−13.7471 ±1.6992 (−0.0893)	−16.9304 ±2.3513 (−1.8480)	−13.5014 ±2.2199 (−5.4446)	6.6314 ±1.1063 (0.8691)	−3.8148 ±1.4460 (2.7405)
$Phr1^{M353A}$	−2.8039 ±5.2827 (13.8117)	−15.0036 ±2.2711 (−1.3458)	−18.2911 ±3.0900 (−3.2087)	−1.3353 ±0.7714 (6.7215)	6.4369 ±1.2070 (0.6746)	−4.8874 ±1.7613 (1.6679)

	E325	W329	N391	Q (M, A) 395	FMN	Adenine
$Cry\text{-}DASH^{wild}$	−1.1246 ±0.9655 (15.491)	−15.5040 ±1.5887 (−1.8462)	−16.9797 ±4.4064 (−1.8973)	−14.8239 ±2.1611 (−6.7671)	7.6132 ±0.9354 (1.8509)	−5.0995 ±1.5737 (1.4558)
$Cry\text{-}DASH^{Q395M}$	−15.0280 ±4.1797 (1.5876)	−13.9541 ±1.9119 (−0.2963)	−16.0027 ±3.0826 (−0.9203)	−7.7569 ±1.1427 (0.2999)	9.0442 ±0.9826 (3.2819)	−6.3781 ±1.2001 (0.1772)
$Cry\text{-}DASH^{Q395A}$	−4.2224 ±5.3027 (12.3932)	−14.8551 ±2.7365 (−1.1973)	−16.1302 ±4.1617 (−1.0478)	−1.1890 ±0.6017 (6.8678)	7.3290 ±1.1694 (1.5667)	−4.5862 ±1.6073 (1.9691)

The interfragment interaction energy (kcal/mol) between each amino acid and the CPD substrate, together with its standard deviation evaluated by the FMO-MP2/6-31G(d) calculations. Differences from that of $Phr1^{wild}$ are shown in parenthesis.

Figure Captions

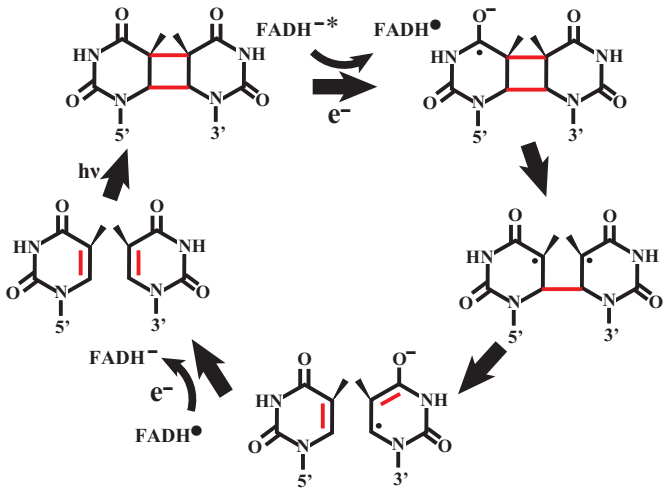

Figure 1. The DNA repair cycle

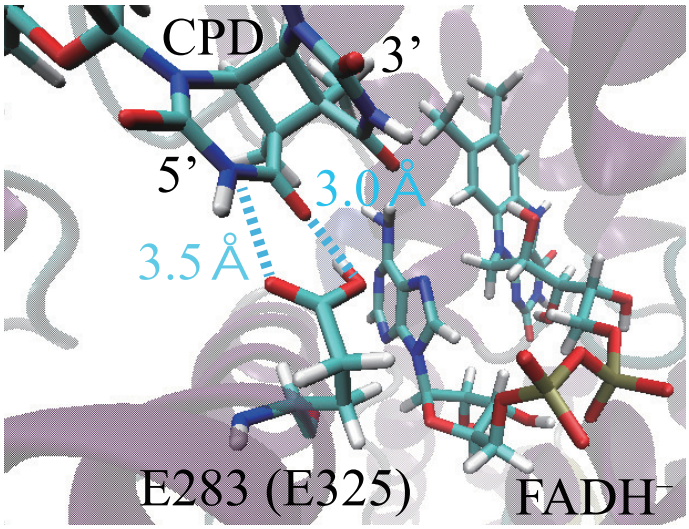

Figure 2. Hydrogen bonds between CPD and E283

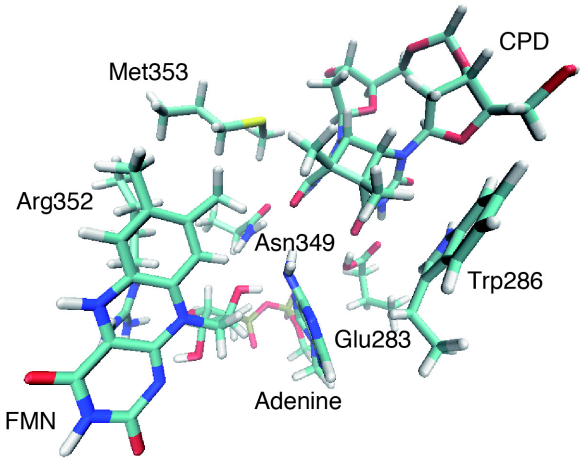

Figure 3. Structure of the QM region

The QM region of the Phr1^{wild} model is shown. In each amino acid residue, the main chain NH and CO groups were replaced by hydrogen atoms.

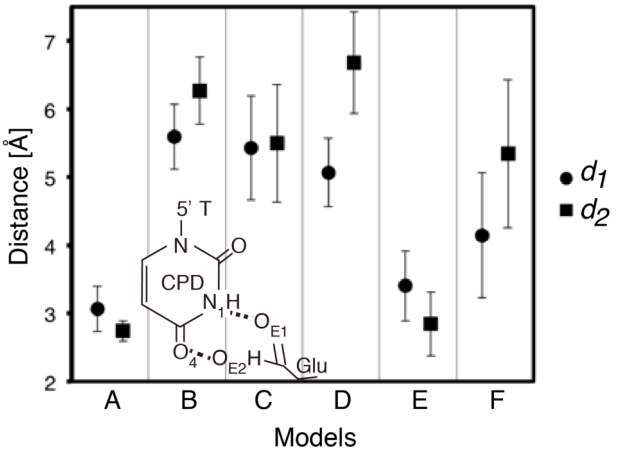

Figure 4. The distance between the CPD and the E-site Glu

The distances between the CPD N1 (O4) proton and the OE1 (OE2) oxygen of the E-site Glu [$d1^{CPD\text{-}E}$ ($d2^{CPD\text{-}E}$)] for the six models [(A) Phr1^{wild}; (B) Phr1^{M353Q}; (C) Phr1^{M353A}; (D) Cry-DASH^{wild}; (E) cry-DASH^{Q395M}; and (F) cry-DASH^{Q395A}] are marked with filled circles (squares): Their average values during the MD simulations, with standard deviations, were 3.061±0.331 (2.741±0.149); 5.593±0.476 (6.268±0.492); 5.430±0.765 (5.497±0.864); 5.067±0.503 (6.680±0.744); 3.402±0.513 (2.846±0.471); and 4.147±0.921 (5.345±1.090) Å, respectively.

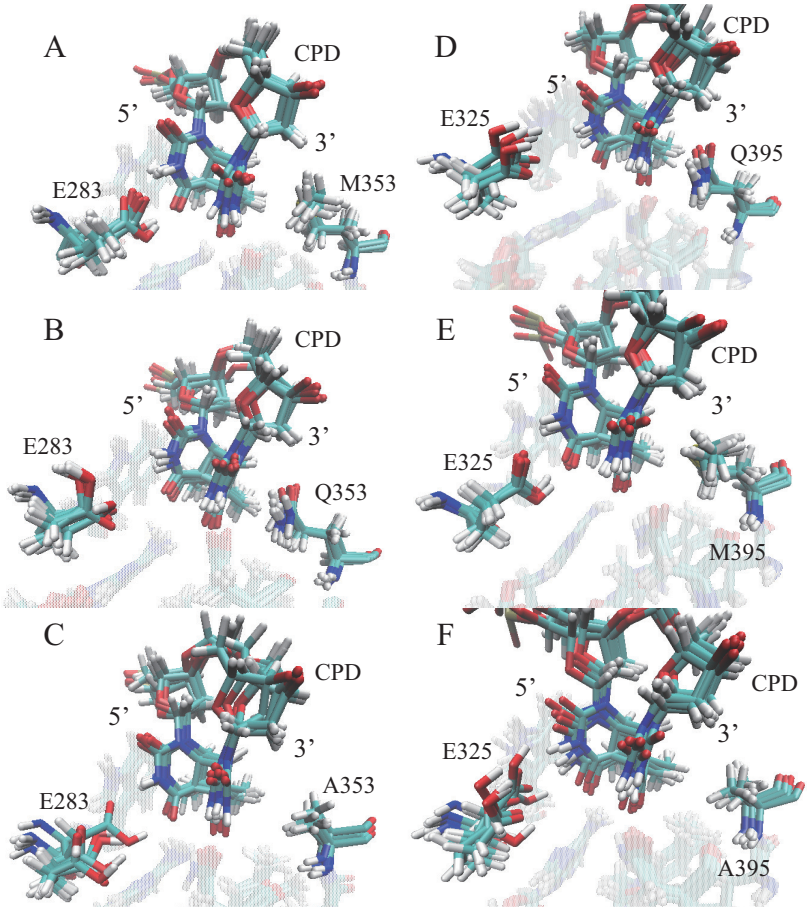

Figure 5. 3D structure of the active site near CPD

Typical simulation snapshots are superimposed for (A) Phr1^{wild}, (B) Phr1^{M353Q}, (C) Phr1^{M353A}, (D) Cry-DASH^{wild}, (E) Cry-DASH^{Q395M}, (F) and Cry-DASH^{Q395A}.

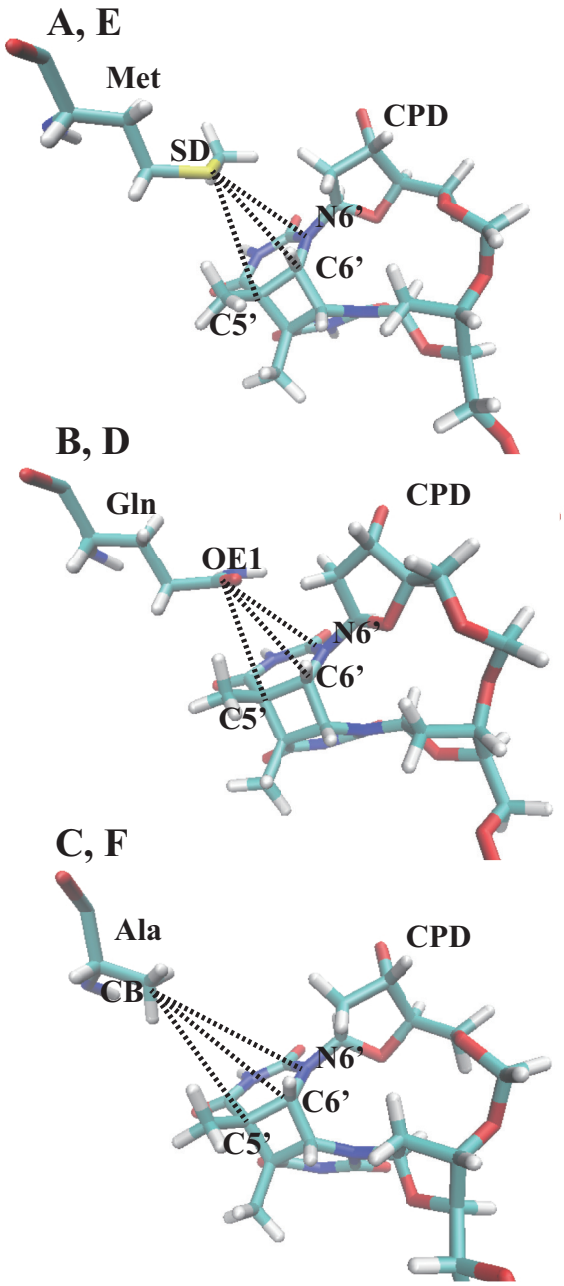

Figure 6. The distance between the CPD and the M-site residue

The distances between the CPD and the M-site residue ($d1^{CPD\text{-}M}$, $d2^{CPD\text{-}M}$, and $d3^{CPD\text{-}M}$) were measured using the interatomic distances between the C5'/C6'/N1 carbon of CPD and the Met SD sulfur (A: Phr^{wild}, E: Cry-$DASH^{Q395M}$), the Ala CB carbon (C: Phr^{M353A}, F: Cry-$DASH^{Q395A}$), or the Gln OE1 oxygen (B: Phr^{M353Q}, D: Cry-$DASH^{wild}$).

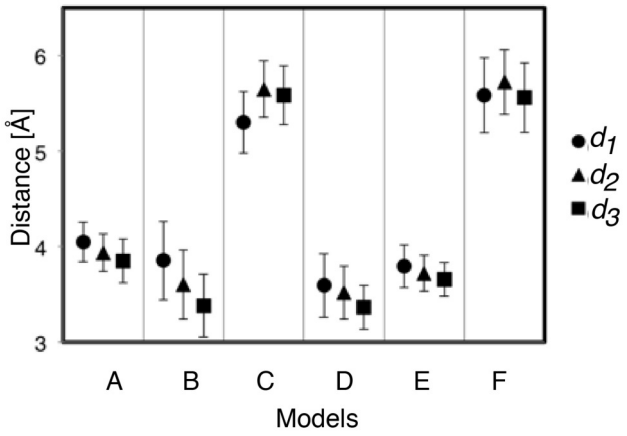

Figure 7. The distance between the CPD and the M-site residue

The distances ($d1^{\text{CPD-M}}$, $d2^{\text{CPD-M}}$, and $d2^{\text{CPD-M}}$) for the six models [(A) $\text{Phr1}^{\text{wild}}$, (B) $\text{Phr1}^{\text{M353Q}}$, (C) $\text{Phr1}^{\text{M353A}}$, (D) $\text{Cry-DASH}^{\text{wild}}$, (E) $\text{Cry-DASH}^{\text{Q395M}}$, and (F) $\text{Cry-DASH}^{\text{Q395A}}$] are marked with filled circles, triangles, and squares, respectively (see Fig. 5). During the MD simulations, their average distances, with standard deviations, of were (4.046±0.208, 3.936±0.196, and 3.851±0.229); (3.855±0.411, 3.602±0.361, and 3.382±0.328); (5.300±0.320, 5.650±0.298, and 5.585±0.310); (3.592±0.331, 3.519±0.280, and 3.362±0.230); (3.795±0.223, 3.722±0.188, and 3.659±0.177); and (5.585±0.394, 5.722±0.339, and 5.561±0.364) Å, respectively.

References

[1] J. Cadet, P. Vigny, The photochemistry of nucleic acids, Bioorganic Photochem. 1 (1990) 1–272.

[2] R. Dulbecco, Reactivation of ultraviolet-inactivated bacteriophage by visible light, Nature. 163 (1949) 949–950.

[3] A. Sancar, Structure and Function of DNA Photolyase and Cryptochrome Blue-Light, Chem. Rev. 103 (2003) 2203–2238.

[4] Y.-T. Kao, C. Saxena, L. Wang, A. Sancar, D. Zhong, Direct observation of thymine dimer repair in DNA by photolyase., Proc. Natl. Acad. Sci. U. S. A. 102 (2005) 16128–16132.

[5] L.O. Essen, T. Klar, Light-driven DNA repair by photolyases, Cell. Mol. Life Sci. 63 (2006) 1266–1277.

[6] F. Masson, T. Laino, U. Rothlisberger, J. Hutter, A QM/MM investigation of thymine dimer radical anion splitting catalyzed by DNA photolyase., Chemphyschem. 10 (2009) 400–10.

[7] J. Antony, D.M. Medvedev, A.A. Stuchebrukhov, Theoretical study of electron transfer between the photolyase catalytic cofactor FADH-and DNA thymine dimer, J. Am. Chem. Soc. 122 (2000) 1057–1065.

[8] D. Medvedev, a a Stuchebrukhov, DNA repair mechanism by photolyase: electron transfer path from the photolyase catalytic cofactor FADH(-) to DNA thymine dimer., J. Theor. Biol. 210 (2001) 237–248.

[9] T.R. Prytkova, D.N. Beratan, S.S. Skourtis, Photoselected electron transfer pathways in DNA photolyase., Proc. Natl. Acad. Sci. U. S. A. 104 (2007) 802–807.

[10] A. Acocella, G. Jones, F. Zerbetto, What is adenine doing in photolyase?, J. Phys. Chem. B. 114 (2010) 4101–4106.

[11] Z. Liu, X. Guo, C. Tan, J. Li, Y.-T. Kao, L. Wang, et al., Electron tunneling pathways and role of adenine in repair of cyclobutane pyrimidine dimer by DNA photolyase., J. Am. Chem. Soc. 134 (2012) 8104–8114.

[12] Y. Miyazawa, H. Nishioka, K. Yura, T. Yamato, Discrimination of class I cyclobutane pyrimidine dimer photolyase from blue light photoreceptors by single methionine residue., Biophys. J. 94 (2008) 2194–2203.

[13] Z. Liu, C. Tan, X. Guo, Y.-T. Kao, J. Li, L. Wang, et al., Dynamics and mechanism of cyclobutane pyrimidine dimer repair by DNA photolyase., Proc. Natl. Acad. Sci. U. S. A. 108 (2011) 14831–14836.

[14] R. Pokorny, T. Klar, U. Hennecke, T. Carell, A. Batschauer, L.-O. Essen, Recognition and repair of UV lesions in loop structures of duplex DNA by DASH-type cryptochrome., Proc. Natl. Acad. Sci. U. S. A. 105 (2008) 21023–21027.

[15] R. Brudler, K. Hitomi, H. Daiyasu, H. Toh, K. Kucho, M. Ishiura, et al., Identification of a new cryptochrome class: structure, function, and evolution, Mol. Cell. 11 (2003) 59–67.

[16] C.P. Selby, A. Sancar, A cryptochrome/photolyase class of enzymes with single-stranded DNA-specific photolyase activity., Proc. Natl. Acad. Sci. U. S. A. 103 (2006) 17696–17700.

[17] Y. Huang, R. Baxter, B.S. Smith, C.L. Partch, C.L. Colbert, J. Deisenhofer, Crystal structure of cryptochrome 3 from Arabidopsis thaliana and its implications for photolyase activity, Proc. Natl. Acad. Sci. 103 (2006) 17701–17706.

[18] A. Mees, T. Klar, P. Gnau, U. Hennecke, A.P.M. Eker, T. Carell, et al., Crystal structure of a photolyase bound to a CPD-like DNA lesion after in situ repair., Science (80-.). 306 (2004) 1789–1793.

[19] N. Senda, Winmostar v. 3.808, Winmoster by Delphi. (n.d.).

[20] J.-H. Lee, C.-J. Park, J.-S. Shin, T. Ikegami, H. Akutsu, B.-S. Choi, NMR structure of the DNA decamer duplex containing double T*G mismatches of cis-syn cyclobutane pyrimidine dimer: implications for DNA damage recognition by the XPC-hHR23B complex., Nucleic Acids Res. 32 (2004) 2474–2481.

[21] W.L. Jorgensen, J. Chandrasekhar, J.D. Madura, R.W. Impey, M.L. Klein, Comparison of simple potential functions for simulating liquid water, J. Chem. Phys. 79 (1983) 926.

[22] D.A. Case, T.A. Darden, T.E. Cheatham III, C.L. Simmerling, J. Wang, R.E. Duke, et al., AMBER 12, Univ. California, San Fr. 1 (2012) 3.

[23] M.J. Frish, G.W. Trucks, H.B. Schlegel, G.E. Scuseria, M.A. Robb, J.R. Cheeseman, Gaussian 03, Gaussian Inc, Wallingford CT. (2003).

[24] K. Kitaura, E. Ikeo, T. Asada, T. Nakano, M. Uebayasi, Fragment molecular orbital method: an approximate computational method for large molecules, Chem. Phys. Lett. 313 (1999) 701–706.

[25] T. Nakano, T. Kaminuma, T. Sato, K. Fukuzawa, Y. Akiyama, M. Uebayasi, et al., Fragment molecular orbital method: use of approximate electrostatic potential, Chem. Phys. Lett. 351 (2002) 475–480.

[26] A. Szabo, N.S. Ostlund, Modern quantum chemistry: introduction to advanced electronic structure theory, Courier Dover Publications, 2012.

[27] D.G. Fedorov, K. Kitaura, Second order Møller-Plesset perturbation theory based upon the fragment molecular orbital method., J. Chem. Phys. 121 (2004) 2483–90.

[28] D.G. Fedorov, K. Kitaura, The importance of three-body terms in the fragment molecular orbital method., J. Chem. Phys. 120 (2004) 6832–40.

[29] M.W. Schmidt, K.K. Baldridge, J.A. Boatz, S.T. Elbert, M.S. Gordon, J.H. Jensen, et al., General Atomic And Molecular Electronic-Structure System, J. Comput. Chem. 14 (1993) 1347–1363.

[30] Z. Liu, C. Tan, X. Guo, Y.-T. Kao, J. Li, L. Wang, et al., Dynamics and mechanism of cyclobutane pyrimidine dimer repair by DNA photolyase., Proc. Natl. Acad. Sci. U. S. A. 108 (2011) 14831–14836.

Supplementary materials

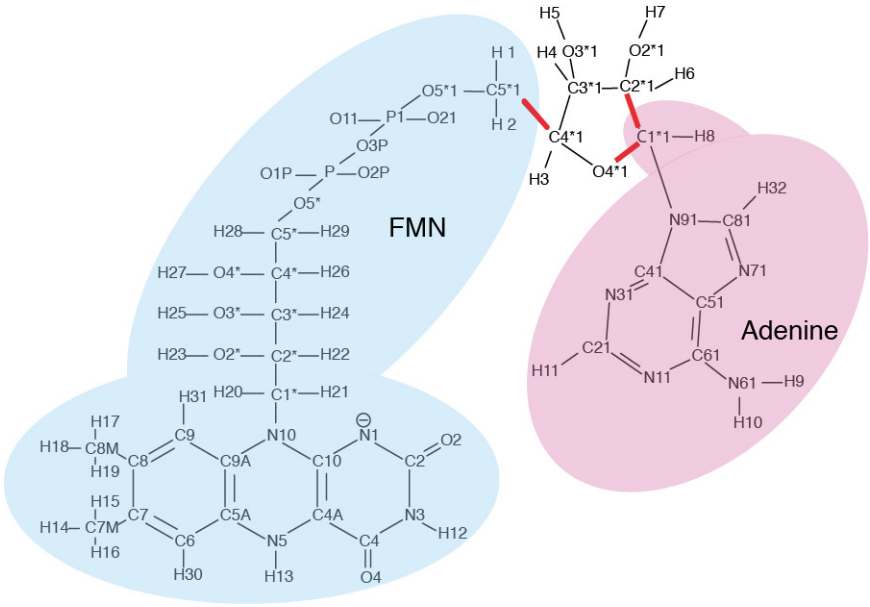

Fig S1. flavin adenine dinucleotide

The flavin mono nucleotide (FMN) and the adenine parts were extracted from the MM model. The three single bonds shown in red were cleaved and the dangling bonds were, then, capped with hydrogen atoms.

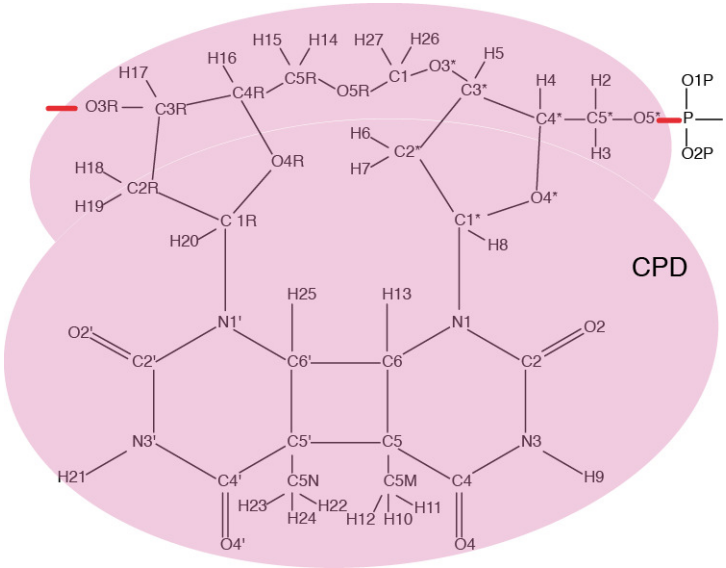

Fig S2. Cyclobutane pyrimidine dimer

The CPD part was extracted from the MM model. The two single bonds shown in red were cleaved and the dangling bonds were, then, capped with hydrogen atoms.